MODELING OF TUNGSTEN MELT LAYER EROSION CAUSED BY JxB FORCE AT TEXTOR WITH THE CODE MEMOS

B. Bazylev[1], J.W. Coenen[2]

[1]Karlsruhe Institute of Technology, IHM, P.O. Karlsruhe, Germany;
[2]Institute of Energy and Climate Research – Plasma Physics, Forschungzentrum Jülich
EURATOM-FZJ, Partner of Trilateral Euregio Cluster, Jülich, Germany

Tungsten in form of macrobrush is foreseen as one of candidate materials for the ITER divertor. Melting of tungsten, the melt motion, and melt splashing are expected to be the main mechanisms of a surface damage determining the lifetime of plasma facing components. Experiments with the long-time plasma action at the metalic surface in a strong magnetic field demonstrated that the JxB force generated by the thermo-emission electrons dominates in the acceleration of the melt layer and leads to a high target damage. In the paper numerical simulation model implemented into the code MEMOS is described and modelling of tungsten target damage caused by the long-time plasma heat loads supporting the TEXTOR experiments are performed with 3D version of the code MEMOS. Calculated damages of tungsten targets are in a reasonable agreement with the target damages observed in the TEXTOR experiments that allows projections upon the surface damage at ITER and DEMO conditions.
PACS: 52.40Hf

INTRODUCTION

Tungsten is foreseen as one of the armour materials for plasma facing components (PFCs) in the ITER divertor and dome and as the main armour material for DEMO. During the transients expected in tokamaks (disruptions, ELMs, and VDE) the armour will be exposed to hot plasma streams and localized impacts of runaway electrons (RE). The heat fluxes are expected to be so high that they can cause severe erosion of PFCs thereby limiting their lifetime. During the intense transients the melting, melt motion, melt splashing and surface evaporation are seen as the main mechanisms of metallic armour erosion [1-5]. In case of RE impact and long time transients (VDE) a melt layer can exist up to several seconds [6]. Experiments at the TEXTOR [7, 8] with the long-time plasma action at the target surface (with duration of few seconds) in a strong magnetic field demonstrated that the JxB force generated by the thermo-emission electrons dominates in the acceleration of the melt layer and leads to a large scale melt motion damage (up to 1 mm per event). Numerical simulations of the TEXTOR experiments with 2D version of the code MEMOS [9] confirmed importance of JxB force as the main driving force causing significant melt motion damage of the tungsten target.

The expected erosion of ITER PFCs under short time transients (with timescale up to few miliseconds) has been properly estimated using the code MEMOS validated against plasma gun target erosion experiments, in which the JxB force is practically negligible [1-5]. The erosion of W target caused by JxB force in short-time plasma action was properly estimated using the code MEMOS and validated against appropriate target erosion experiments at the plasma gun facility QSPA Kh-50 [10]. Simulations of the long-time interaction of a plasma with the tungsten limiter in the TEXTOR experiments [11], demonstrated that Richardson-Dushman expression used in the code MEMOS significantly overestimated the thermo-electron emission as well the code MEMOS has to be significantly upgraded to simulate large scale melt layer displacement observed in the TEXTOR experiments.

To simulate the TEXTOR experiments with the large scale melt layer displacements the code MEMOS was significantly updated, in particular acquiring some additional 3D features of the experimental conditions. The 3D simulation model implemented into the code MEMOS is described. New models of the space-charge limited thermo-emission were implemented into the code. In the paper new MEMOS simulations for the TEXTOR experiments on tungsten target damage under long-time plasma heat loads with heat fluxes measured TEXTOR experiments ($Q \sim 15...30$ MW/m^2) on the timescale of 5...6 s in a strong magnetic field are performed, with taking into account 3D geometrical peculiarities of the experiments. The melt layer damage is calculated for single shot using 3D version of the code MEMOS. Calculated damages of tungsten targets are in a reasonable agreement with the target damages observed in the TEXTOR experiments.

1. EROSION OF TUNGSTEN TARGET IN TEXTOR EXPERIMENT. SIMULATIONS VS EXPERIMENT

1.1. RESULTS OF TEXTOR EXPERIMENTS

Experiments have been performed by introducing a limiter into plasma at TEXTOR. Experimental conditions in more detail are described in [7, 8]. One Shot experiments was performed for the un-castellated target with sizes 3.5x5.5x0.2 cm (with the following coordinate system: Z - (poloidal direction), Y, X - (thickness of the target)); irradiated area along Y direction is about 2.5 cm. The upper part of the tungsten sample can receive up to $Q \sim 45$ MW/m^2 for leading edges. The typical heat flux is about $Q \sim 20...25$ MW/m^2 for plasma load duration of 5...6 s. The peak temperatures are about 4000 K. The heat fluxes and surface temperature along leading edge (along poloidal direction) of the limiter was measured with high time resolution (Figs. 1, 2). The heat fluxes were measured with the large shot noise therefore the averaging along poloidal direction was done and average flux is demonstrated on Fig. 1. Constant temperature level after

2 s and decreasing of the heat flux at the surface are observed in experiments (see Figs. 1, 2). These effects are caused by the plasma shielding of evaporated tungsten [9]. Typical melt layer thickness observed in experiments is about 1...1.5 mm. Typical erosion of the tungsten brushes caused by the JxB force generated by thermo-emission electrons in the strong magnetic field (B = 2.25 T) after single shot can reach few mm. The thermo-emission current density estimated in the experiments is about several tens A/cm^2. The final surface of the damaged W target is demonstrated in Fig. 3.
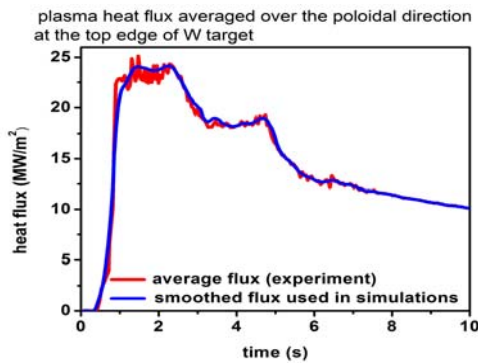

Fig. 1. The time dependencies of plasma heat flux along poloidal direction at the top edge of the target
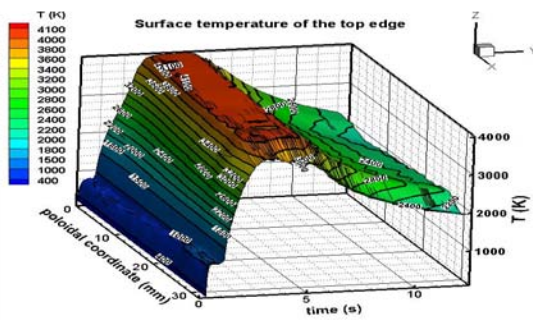

Fig. 2. Measured time dependencies of surface temperature along poloidal direction at the top edge of the target (TEXTOR experiment)
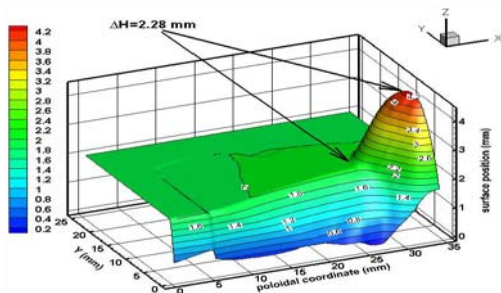

Fig. 3. Final surface profile of the W target after resolidification (TEXTOR experiment)

1.2. NUMERICAL SIMULATIONS

The code MEMOS [1] significantly upgraded to 3D geometry have been applied for numerical simulations of the melt motion damage experiments carried out at the TEXTOR [7, 8]. The main features of the numerical model introducing into the code are described in Chapter 2.
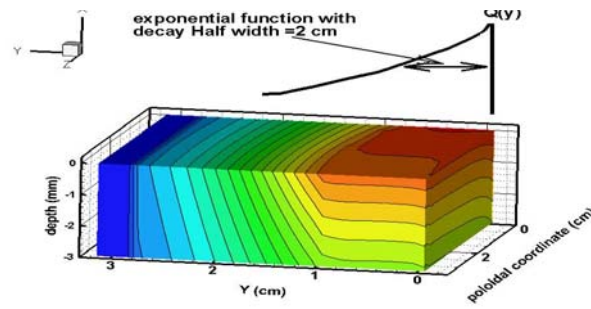

Fig. 4. Sketch of the target used in the 3D simulations

The numerical simulations of the TEXTOR experiments were carried out for the tungsten un-castellated targets preheated up to 200°C using 3D version of the code MEMOS. The geometry of the numerical simulation is demonstrated at the sketch (Fig. 4): with sizes 3.5x3.2x0.3 cm (Z(poloidal), Y, X(thickness)); irradiated area along Y direction is about 2.5 cm. The heat flux along poloidal direction is assumed to be constant using smoothed experimental flux (Fig. 1). Along Y direction exponential function of flux decay is assumed. Several scenarios with different maximum heat load Q ranged between 21 and 27 MW/m^2 are calculated. The plasma pressure at the target were p=200 Pa (as at the TEXTOR experiments), magnetic field B=2.25 T the Child-Langmuir expression is used for calculation of the thermo-emission current. It is also assumed that the back side of the tungsten target is cooled radiatively.
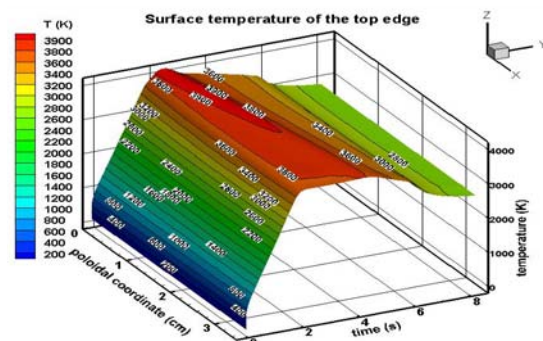

Fig. 5. Calculated time dependencies of surface temperature along poloidal direction at the top edge of the target Q_{max}=25 MW/m^2 (MEMOS simulation)

Let us illustrate physical processes of plasma tungsten interaction in the TEXTOR experiments. Impacting plasma heats the tungsten target after approximately 1 s surface temperature exceeds the melting temperature and then after approximately 2 s the temperature becomes high enough for starting significant evaporation. Tungsten evaporated from the target produces plasma shielding above the surface leading to the noticeable surface screening from the impacting plasma: absorbed flux significantly drop down, and the surface temperature stabilizes at T ~ 4000 K (see Fig. 2 and Fig. 5). Typical calculated thickness of a melt layer is about 1.3…1.5 mm that is in a rather good agreement with the measured data.
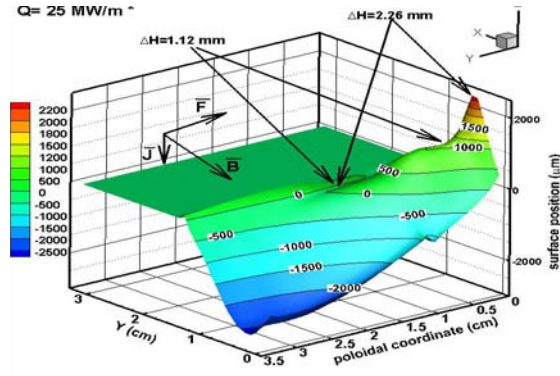
4

Fig. 6. Calculated final surface profile of the W target after resolidification (MEMOS simulation)

Simulations of brush erosion caused by the JxB force for the several heat load scenarios Q_{max} ranged between 21 and 27 MW/m^2 witth given timescale of 6 s demonstrates large scale displacement of the melt layer and significant target damage. Typical maximal amplitudes of the thermo-emission current calculated by new model are about 30…40 A/cm^2. The JxB force generates melt layer motion with velocities of about several tens cm/s. The final damages of the tungsten brushes (Fig. 6) are of 2 mm for scenario Q = 25 MW/m^2. Comparison of the final calculated turget damages with the measured ones (compare Figs. 3 and 6) demonstrates reasonable agreement between the numerical simulations and the TEXTOR experiments. Dependance of the surface damage on maximum heat loads is demonstrated on Fig. 7.
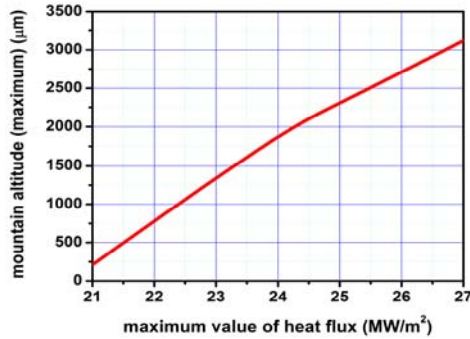

Fig. 7. Calculated dependence of maximum mountain altitude on the maximum heat loads Q_{max}

2. THE MODEL FOR MELT MOTION

In the code MEMOS motion melted material along the surface is described in the 'shallow water' approximation of the Navier-Stokes equations, with the surface tension, viscosity of molten metal, and the radiative losses from the hot surface taken into account. The plasma pressure gradients along the divertor plate, as well as the gradient of surface tension and the JxB force of the currents crossing the melt layer immersed in a strong magnetic field, produce the melt acceleration.

For a derivation of the mathematical model for melt motion the following assumptions are used here: the thicknessof the melt layer is much smaller than the width of the molten layer and pressure gradients across the melt layer are absent. Therefore there exists only a velocity component parallel to the surface and a melt

velocity averaged over the molten layer can be used for description of the melt motion. In this case the "shallow water" approximation can be applied for the mathematical description of the melt motion [13]. The fluid is assumed to be incompressible. Temperature dependent thermo-physical data are used. The physical processes taken into account in the numerical model are: heating, melting, evaporation from the surface and resolidification, heat transport in the liquid and the solid, viscosity and melt motion by the following forces: surface tension, total external pressure, Lorentz force due to external and Eddy currents.

The base system of Navier-Stocks equations [4] together with the heat conductivity equation describe the problem (coordinate system in Fig. 4):

$$\text{div } \mathbf{v} = 0 , \tag{1}$$

$$\rho\left(\frac{\partial \mathbf{v}}{\partial t} + \mathbf{v}\nabla\mathbf{v}\right) = -\text{grad } p + \mu\,\Delta\mathbf{v} + F_{Lorentz} , \tag{2}$$

$$\rho C \frac{\partial T}{\partial t} + \mathbf{v}\,\text{grad}\,T = \nabla(\kappa\,\nabla T) + Q , \tag{3}$$

with $\mathbf{v}, T, \rho, C, \kappa$ velocity, temperature, density, specific heat and heat conductivity, μ viscosity of the melt, p is pressure, Q is sum of volumetric energy deposition and Joule heating. The following boundary conditions are applied at the liquid vapor boundary:

$$-\kappa \frac{\partial T}{\partial n}\bigg|_{surf} = W(t) - \rho V_{ev}\Delta H_{ev}, \tag{4}$$

$$\mu \frac{\partial u_y}{\partial z} = \frac{\partial \alpha}{\partial y}, \qquad \mu \frac{\partial u_z}{\partial z} = \frac{\partial \alpha}{\partial z}, \tag{5}$$

here in (4) temperature gradient is calculated at the surface along the normal, $W(t)$ is surface heat load, ΔH_{ev} is enthalpy of evaporation. In (5) u_y, u_z is velocity component along the surface, α is surface tension coefficient. The classic Stefan boundary condition is applied to the solid liquid boundary. At the melting front ($n = N_m$) the velocity of the melt motion assumed to be zero here n is normal to the melt front.

$$\kappa_s \frac{\partial T_s}{\partial n}\bigg|_{n=N_m} - \kappa_l \frac{\partial T_l}{\partial n}\bigg|_{n=N_m} = \rho V_m \Delta H_m , \tag{6}$$

here index s refers to the solid and index l to the liquid phase, V_m is velocity of melting front propagation, ΔH_m is enthalpy of melting.

The shallow water approximation allows to simplify the system of Eqs. (1)–(3) with the boundary conditions (4)–(6) to a system of quasi 2-D equations. The fluid velocity is averaged over the melt layer thickness assuming a parabolic dependence. After averaging Eqs. (1) and (2) with the boundary condition (Eq. (5)) the system of equation of the St. Venant type [7] is derived:

$$\frac{\partial h}{\partial t} + \frac{\partial(u_y h)}{\partial y} + \frac{\partial(u_z h)}{\partial z} = V_{ev} + V_m , \tag{7}$$

$$\frac{\partial u_y}{\partial t} + u_y \frac{\partial u_y}{\partial y} = -\frac{1}{\rho}\frac{\partial p}{\partial y} - \frac{u_y}{h}V_m + \nu \frac{\partial^2 u_y}{\partial y^2} -$$
$$3\nu \frac{u_y}{h^2} + \frac{3k_\alpha}{2\rho h}\frac{\partial T}{\partial y} + \frac{J_z B_y}{\rho c}, \qquad (8)$$

$$\frac{\partial u_z}{\partial t} + u_z \frac{\partial u_z}{\partial z} = -\frac{1}{\rho}\frac{\partial p}{\partial z} - \frac{u_z}{h}V_m + \nu \frac{\partial^2 u_z}{\partial z^2} -$$
$$3\nu \frac{u_z}{h^2} + \frac{3k_\alpha}{2\rho h}\frac{\partial T}{\partial z} + \frac{J_y B_z}{\rho c}. \qquad (9)$$

Here ν is the kinematic viscosity, J_z, J_y component of the current, B_y, B_z the toroidal magnetic field components, T melt temperature, and instead of α the negative coefficient given by $k_\alpha = \partial \alpha / \partial T$ is used, V_{ev} velocity of the surface caused by the evaporation. The equations describing the evolution of the normal velocity at the surface V_{sf} and the heat transport along the surface remain also intact:

$$V_{sf} = V_{ev} - \frac{\partial(u_y h)}{\partial y} - \frac{\partial(u_z h)}{\partial z}, \qquad (10)$$

$$\frac{\partial T}{\partial t} + u_y \frac{\partial T}{\partial y} + u_z \frac{\partial T}{\partial z} = \frac{3\nu}{C}\frac{u_y^2}{h^2} + \frac{3\nu}{C}\frac{u_z^2}{h^2}. \qquad (11)$$

The 3D Stefan problem Eq. (3) for moving boundaries attached to re-solidification, melting and vaporization fronts is solved using the splitting method.

As it was mentioned, the melt motion is generated by the thermo-emission current in the TEXTOR experiments. For a good agreement with the experiment the model of space-charge limited thermo-emission current based on the modified Child-Langmuir expressions [12] is implemented into the code MEMOS instead of Richardson-Dushman formula. Free parameters entering into the expressions are fitted so that calculated current is in a correlation with the experimental values. A 3D heat transport equation with two boundary conditions at the moving vapor-liquid- and liquid-solid interfaces describes the temperature inside the target. Temperature dependent thermo-physical data are used [14]. The model of the plasma shielding well developed, validated against experiments at plasma gun facilities, and described in details in ref. [15] have been implemented into the code MEMOS to take into account influence of the evaporated material on the surface heat loads.

CONCLUSIONS

To simulate long-time plasma action at the tungsten surface and large space scale melt motion in TEXTOR experiments the code MEMOS was significantly updated to 3D geometry, in particular accounting for some additional 3D features. The thermo-emission current model was improved accounting for space charge limitation.

Results of numerical simulations carried out for the heat loads in the range 21...27 MW/m^2 on the timescale of 5...6 s have demonstrated a reasonable agreement with TEXTOR experimental data on time dependents of surface temperature, and on tungsten target erosion.

The JxB force, generated by the thermo-emission current, becomes important in melt motion damage for the long-time transients such as VDE and runaway electron impact in which melt layer can exist till few seconds

Further numerical simulations of the TEXTOR single pulse and multi-pulse experiments using 2D and 3D version of the code MEMOS have to be further performed.

REFERENCES

1. B. Bazylev, H.Wuerz // *J. Nucl. Mater.* 2002, v. 307-311, p. 69.
2. B. Bazylev et al. // *J. Nucl. Mater.* 2005, v. 337-339, p. 766-770.
3. B. Bazylev et al. // *Fusion Eng. Des.* 2009, v. 84, iss 2, p. 441.
4. B. Bazylev et al. // *J. Nucl. Mater.* 2007, v. 363-365, p. 1011-1015.
5. B. Bazylev et al. // *J. Nucl. Mater.* 2009, v. 386-388, p. 919-921.
6. B. Bazylev et al. // *J. Nucl. Mater.* 2011, v. 417, p. 655-658.
7. J.W. Coenen et al. // *J. Nucl. Mater.* 2011, v. 415, S78.
8. J.W. Coenen et al. // *Nuclear Fusion.* 2011, v. 51, p. 083008 (11 p.).
9. B.B. Bazylev et al. // *Physica Scripta* 2011, v. T145, p. 014054.
10. I.E. Garkusha et al. // *J. Nucl. Mater.* 2007, v. 363-365, p. 1021.
11. G. Sergienko et al. // *J. Nucl. Mater.* 2007, v. 363-365, p. 96.
12. S. Takamura et al. // *Contrib. Plasma Phys.* 2004, v. 44, № 1-3, p. 126.
13 L.D. Landau, E.N. Lifshits // *Fluid Mechanics, Pergamon.* New York, 1959.
14. Y.S. Touloukian (ed). *Thermophysical Properties of Materials.* New York, 1970.
15. H. Wuerz et al. // *Fusion Science and Technology.* 2001, v. 40, p. 191.

МОДЕЛИРОВАНИЕ ЭРОЗИИ РАСПЛАВЛЕННОГО СЛОЯ ВОЛЬФРАМА, ОБУСЛОВЛЕННОЙ J×B-СИЛОЙ, В TEXTORe КОДОМ MEMOS

Б. Базылев, J.W. Coenen

Вольфрам в виде макробрашей рассматривается в качестве основного материала для дивертора ИТЭРа. Плавления вольфрама, движение и разбрызгивание расплава рассматриваются в качестве основных механизмов повреждения поверхности, которые определяют время жизни элементов дивертора. Эксперименты с длительным воздействием плазмы на металлические поверхности в сильном магнитном поле показали, что JxB-сила, генерируемая термоэмиссией электронов, доминирует в ускорении слоя расплава и приводит к большому повреждению поверхности. Описана численная модель моделирования эрозии металлической поверхности при плазменном воздействии, имплементированная в код MEMOS. Приведены результаты моделирования эрозии вольфрамовой мишени, вызванной длительным воздействием плазмы в экспериментах в TEXTORe, проведенного 3D-версией кода MEMOS. Расчетная эрозия вольфрама находится в разумном согласии с эрозией вольфрамового лимитера, которая наблюдалась в экспериментах в TEXTORe. Данные расчета позволяют делать прогнозы относительно эрозии поверхности в условиях ИТЭР и ДЕМО.

МОДЕЛЮВАННЯ ЕРОЗІЇ РОЗПЛАВЛЕНОГО ШАРУ ВОЛЬФРАМУ, ЗУМОВЛЕНОЇ J×B-СИЛОЮ, В TEXTORi КОДОМ MEMOS

Б. Базилєв, J.W. Coenen

Вольфрам у вигляді макробрашів розглядається в якості основного матеріалу для дивертора ІТЕРа. Плавлення вольфраму, рух і розбризкування розплаву розглядаються в якості основних механізмів пошкодження поверхні, що визначають час життя елементів дивертора. Експерименти з тривалим впливом плазми на металеві поверхні в сильному магнітному полі показали, що JxB-сила, що генерується термо-емісією електронів, домінується в прискоренні шару розплаву і приводить до великих пошкоджень поверхні. Описана чисельна модель моделювання ерозії металевої поверхні при плазмовому впливі, імплементована в код MEMOS. Наведено результати моделювання ерозії вольфрамової мішені, викликаної тривалим впливом плазми в експериментах в TEXTORi, проведенного 3D-версією коду MEMOS. Розрахункована ерозія вольфраму знаходиться в розумній згоді з ерозією вольфрамового лімітера, яка спостерігалася в експериментах в TEXTORi. Дані розрахунку дозволяють робити прогнози, щодо ерозії поверхні в умовах ІТЕР і ДЕМО.